Resource Operators Conference

Faculty of Engineering and Information Sciences

2022

Numerical analysis of strain energy density at development and longwall face

Chunchen Wei
University of New South Wales

Onur Vardar
University of New South Wales

Chengguo Zhang
University of New South Wales

John Watson
University of New South Wales

Ismet Canbulat
University of New South Wales

Follow this and additional works at: https://ro.uow.edu.au/coal

NUMERICAL ANALYSIS OF STRAIN ENERGY DENSITY AT DEVELOPMENT AND LONGWALL FACE

Chunchen Wei[1,*], Onur Vardar[1], Chengguo Zhang[1], John Watson[1] and Ismet Canbulat[1]

ABSTRACT: Strain energy stored within coal mass is one of the main energy sources of coal bursts. Damage caused by a coal burst event can be attributed to the magnitude of strain energy accumulated around excavations. In this study, strain energy density (SED) within coal seam is examined around excavation boundaries during development and longwall retreat. Several numerical models are generated to investigate SED distributions for mining depths ranging between 100 m and 1000 m. For both development and longwall retreat, the maximum SED area migrated deeper into excavation boundaries with increasing mining depth. When the mining depth increased from 100 m to 1000 m, the maximum SED around development increased from approximately 6 kJ/m3 to 780 kJ/m3, while the maximum SED at longwall face increased from approximately 102 kJ/m3 to 1710 kJ/m3. The maximum SED around roadway ribs was lower than that at longwall face at the same mining depth. The sensitivity analyses presented in this study can provide guidance to geotechnical engineers to better understand and evaluate associated risks for different mining conditions.

INTRODUCTION

Rockburst is a dynamic form of rock failure, where the broken rock material is ejected into underground excavations in the form of strain burst, ejection or bulking, resulting in damage and/or personnel injuries. Rockburst has been regarded as a major challenge in especially deep underground excavations for decades. The term 'coal burst' refers to rockburst that occurs in underground coal excavations (Hebblewhite and Galvin, 2017). Coal burst occurs under the effects of complex environments of geological and geotechnical mining conditions (Iannacchione and Tadolini, 2016; Zhang et al., 2017; Vardar et al., 2018). Nevertheless, a major component of coal burst mechanism is associated with energy storage and release.

A strain burst is a form of rockburst. A small change in the stress field and/or material strength can result in a strain burst where the strain energy stored in the rock mass is released in an unstable and violent manner. Galvin (2016) pointed out that strain bursts occur due to the localised strain energy concentrations near excavation boundaries. Thus, it is critical to examine the distribution of strain energy density around excavations during development and longwall retreat.

In this study, the Universal Distinct Element Code (UDEC) is applied to investigate the strain energy density around roadway rib and longwall face during excavations. A range of parametric analyses is conducted to assess the role of the contributing factors.

NUMERICAL MODEL SET-UP

Model configuration and mechanical properties
For both the longwall and development roadway models, the coal seam thickness and mining height are taken as 3 m, and the immediate roof is of thickness 10 m. For the longwall model, the thickness of the floor is 200 m, a main roof layer is sitting above the immediate roof and the total thickness of roof material (above the coal seam) is equal to the mining depth. In the roadway model, the main roof is 20m thick and the floor 30m thick. The geometries and boundary conditions of the longwall and development roadway models are shown in **Figure 1** and **Figure 2**, respectively. For both models the blocks are deformable and the zone size within blocks is 0.5 m by 0.5 m in the coal seam, increasing gradually through the rock to the outer boundaries. A plane strain condition exists for both the longwall and

---

development models, so the UDEC longwall model represents a thin slice in the middle of the face during longwall retreat. Roller boundary conditions are applied to the vertical sides of the models, and fixed boundary conditions to the bottom.
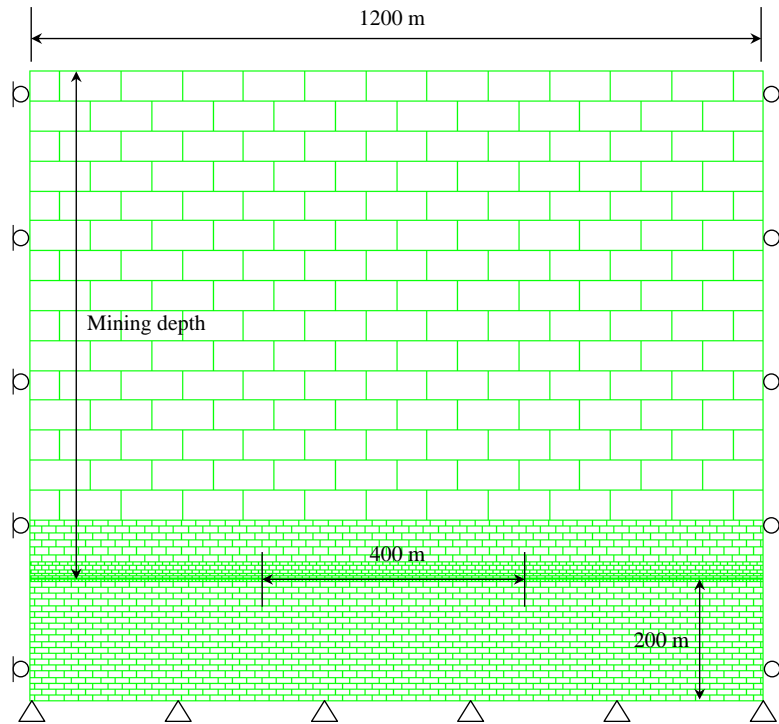

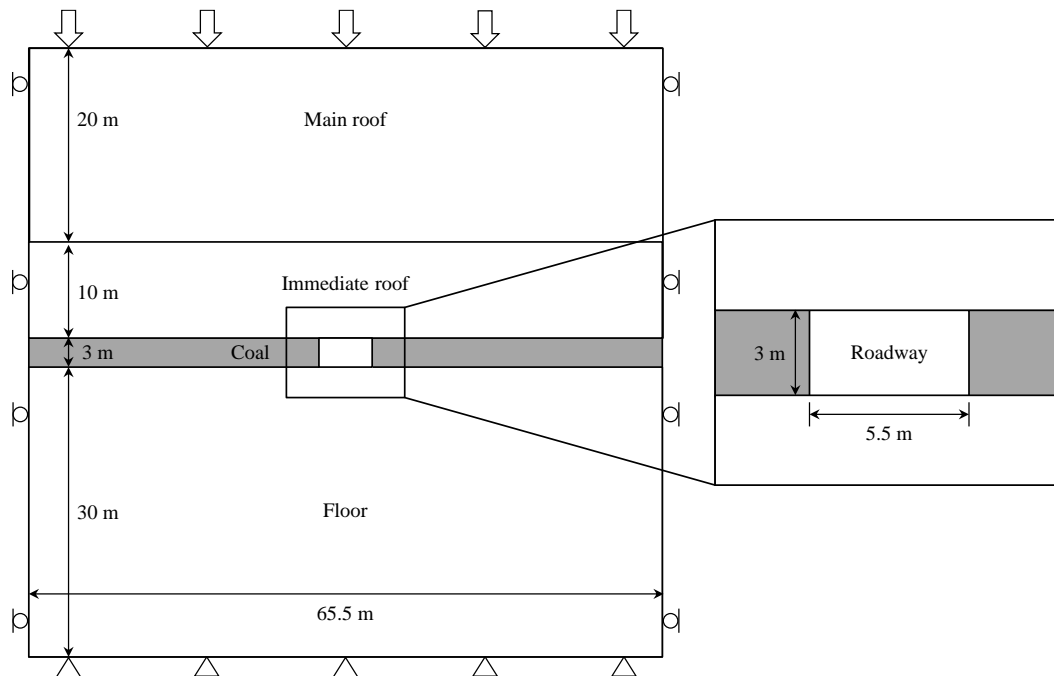**Figure 1: The longwall model geometry and boundary conditions**

Figure 2: The roadway model geometry and boundary conditions (not to scale)

The mechanical properties taken for the rock units (*i.e.* UDEC deformable blocks) in the longwall and roadway development models are listed in **Table 1**. The Mohr-Coulomb strain-softening (MCSS) constitutive model is used for all rocks. Once a compressive failure takes place, the material cohesion is linearly reduced to its residual value over a plastic strain of 0.05 and kept constant beyond that critical strain value (Wang et al., 2011; Lorig and Varona, 2013; Shen et al., 2019; Vardar, 2019). The material friction angle, on the other hand, is assumed to be constant (35°) for rocks in roof and floor. A tensile

strength to uniaxial compressive strength (UCS) ratio of 0.1 is taken for the rocks and the residual tensile strength dropped to zero after a 0.001 plastic strain in tension. Lastly, a UCS (in MPa) to Young's modulus (in GPa) ratio of three is assumed to model the rocks in roof and floor (Zipf, 2006; Vardar, 2019).

Table 1: Mechanical properties taken for rock units

Rock units	UCS (MPa)	E (GPa)	Poisson's ratio
Coal mass	6.6	2	0.25
Immediate roof	24	8	0.25
Main roof and floor	36	12	0.25

In this study, the bedding planes and vertical joints are modelled using a Coulomb-slip constitutive model. The friction angles are 25°; while the cohesion or tensile strength values are taken as zero(Zipf, 2006; Wei et al., 2021). **Table 2** lists the properties taken for the bedding planes (both in rock and coal) and the vertical joints in this study.

Table 2: Coulomb-slip properties taken for the discontinuities in the analysis

Discontinuity type	Normal stiffness (GPa/m)	Shear stiffness (GPa/m)	Peak friction angle (°)	Cohesion (MPa)	Tensile strength (MPa)
Bedding plane	50	5	25	0	0
Joints	50	5	25	0	0

In the analyses, six different mining depth scenarios are simulated: 100 m, 300 m, 500 m, 700 m, 850 m, 1000 m. The maximum horizontal stress is perpendicular to the longwall panel, and its magnitude is assumed to be two times the vertical stress. The minimum horizontal stress magnitude is equal to the magnitude of vertical stress (Vardar, 2019; Wei et al., 2020).

The coal properties are determined by correlation of the results of strain softening analysis with the Salamon and slender pillar formulae for coal pillar strength for the range of width to height ratios 1.0 to 5.0, as given by Equation (1). The calibrated coal properties are given in **Table 3**.

$$\sigma_{ps} = 8.60 \frac{w^{0.51}}{h^{0.84}} \tag{1}$$

where σ_{ps} is the strength (average vertical stress at collapse) of the pillar, and *w* and *h* are the pillar width and height in metres, respectively.

Table 3: Mechanical properties taken for coal mass

Property	Peak	Residual	Critical plastic strain
Cohesion	2.2 MPa	0.2 MPa	0.06
Friction angle	23°	23°	-
Tensile strength	0.5 MPa	0	0.001

The calibration process also produces a coal mass compressive strength of approximately 6.65 MPa. This value is obtained using the following equation:

$$UCS = \frac{2c\cos(\phi)}{1-\sin(\phi)} \tag{2}$$

where *c* is cohesion while ϕ is friction angle.

Quantification of strain energy density (SED)

Strain energy is calculated on the basis of the rock mass properties and stress environment. The strain energy density (SED) stored within the rock mass surrounding excavations is quantified by a user-defined FISH program using Equation (3).

$$SED = \frac{1}{2E}\left[(\sigma_1^2 + \sigma_2^2 + \sigma_3^2) - 2v(\sigma_1\sigma_2 + \sigma_1\sigma_3 + \sigma_2\sigma_3) \right] \qquad (3)$$

where E is Young's Modulus; v is Poisson's ratio; and σ_1, σ_2, σ_3 are the principal stress components. Commonly, the unit of SED used for underground coal mining is kJ/m^3. Therefore, in the following sections, kJ/m^3 is used consistently for SED measurement.

According to Equation (3), the pre-mining strain energy density expected within a coal seam at a given depth is as shown in **Table 4**.

Table 4: Strain energy densities within coal seam at various depths

Mining depth (m)	100	300	500	700	850	1000
SED (kJ/m^3)	5.5	49.2	136.7	268.0	395.1	546.9

MODEL RESULTS AND DISCUSSION

Strain energy density during Longwall retreat

In the longwall model, the panel is excavated for a distance of 400m, as shown in **Figure 1**. The strain energy density ahead of the longwall face is calculated at the end of the longwall retreat for each mining depth. **Figure 3** illustrates the strain energy density ahead of the longwall face in 700m of mining depth, where the maximum SED area is approximately 7.7 m in front of the longwall face. The maximum SED is approximately 1070 kJ/m^3. The coal mass between the maximum SED point and the longwall face is generally in a yielded state, in which the SED is less than that stored in the coal seam before mining (i.e., *in situ* state). The average SED in the yielded coal (between the longwall face and the maximum SED area) is approximately 58.9 kJ/m^3 in the 700 m depth of mining model.
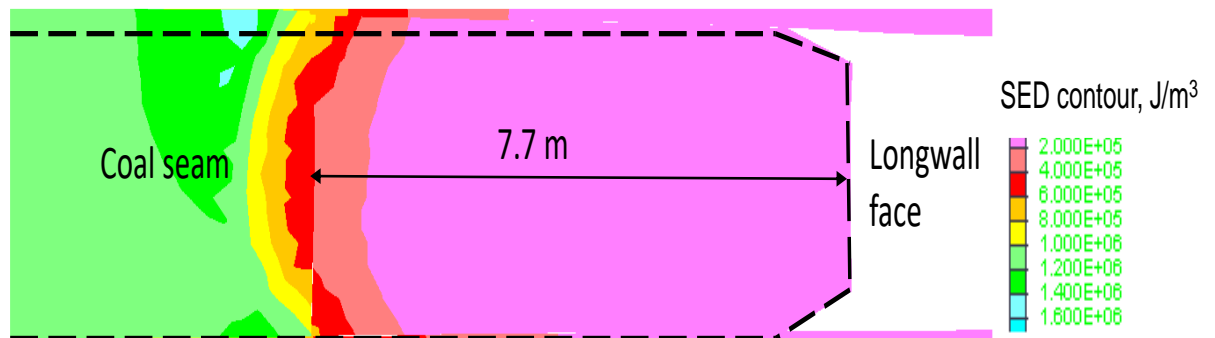

Figure 3: An example of strain energy density contours in the coal seam at the face for 700m mining depth (with deformable mesh)

The average SED in the yielded coal seam in various mining depths is shown in **Figure 4**. It shows that the average SED in yielded coal increases linearly from 10.5 kJ/m^3 in 100 m depth of mining to 95.7 kJ/m^3 in 1000 m depth of mining. The average SED in 1000 m mining depth is approximately ten times the average SED in 100 m mining depth.

As shown in **Figure 5**, the maximum SED area migrates deeper into the longwall face with increasing mining depth. The distance increases drastically from 3 m to 6 m when the mining depth increases from 100 m to 300 m. Then it increases slowly up to 8m at 1000m mining depth.

In **Figure 6**, the maximum SED around longwall face is summarised for various mining depths. **Figure 6** also compares the maximum SED to that of the coal seam in the *in situ* stress state, of which values are listed in **Table 4**. It is clear that the strain energy stored in the coal seam increases after the longwall excavation. The difference of SED before and after longwall excavation increases with increasing mining depth. This means that the strain energy stored around the excavation increases with increasing mining

depth. The maximum SED is approximately 1710 kJ/m^3 ahead of the longwall face when the mining depth is 1000 m.
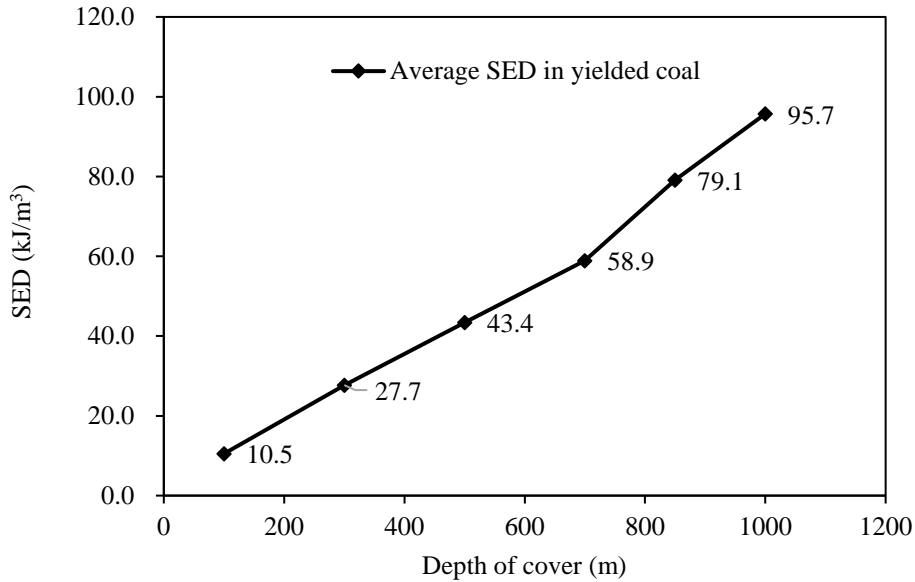

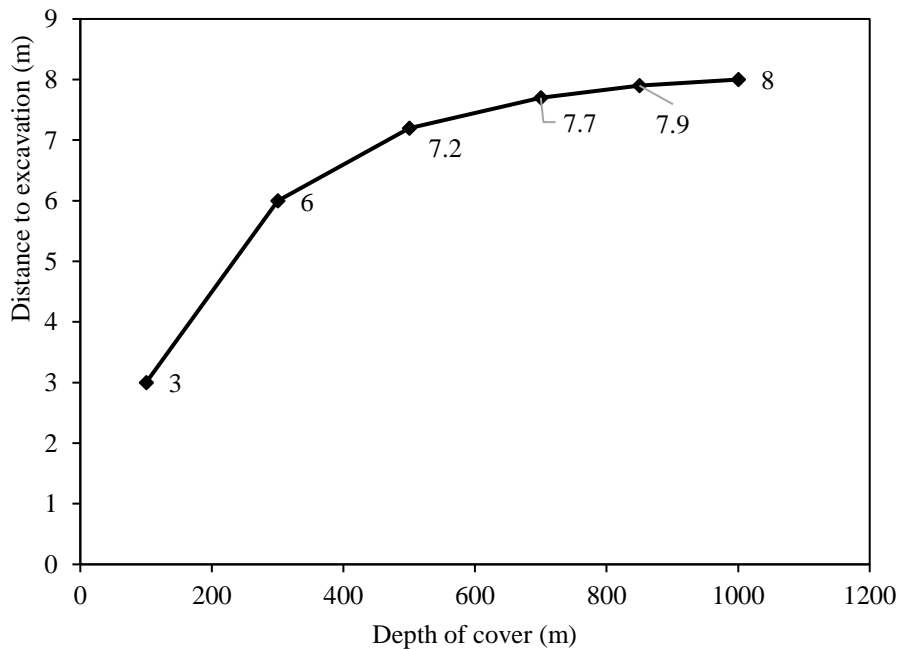**Figure 4: Average SED in yielded coal seam at various mining depth at LW face**

Figure 5: The position of maximum SED area ahead of LW face

In 100 m mining depth, the maximum SED (102 kJ/m^3) is 9.7 times the average SED (10.5 kJ/m^3) in the yielded coal face. In addition, the maximum SED increases to approximately eighteen times the average SED in the yielded coal when the depth of mining is in a range of 700 m to 1000 m. It indicates that a large portion of strain energy is stored within the elastic coal in front of the longwall face due to the abutment stress. The coal at the longwall face has a limited amount of strain energy due to the yielding state. Thus, the elastic strain energy stored in the elastic coal is highly likely one of the main energy sources when strain bursts occur.
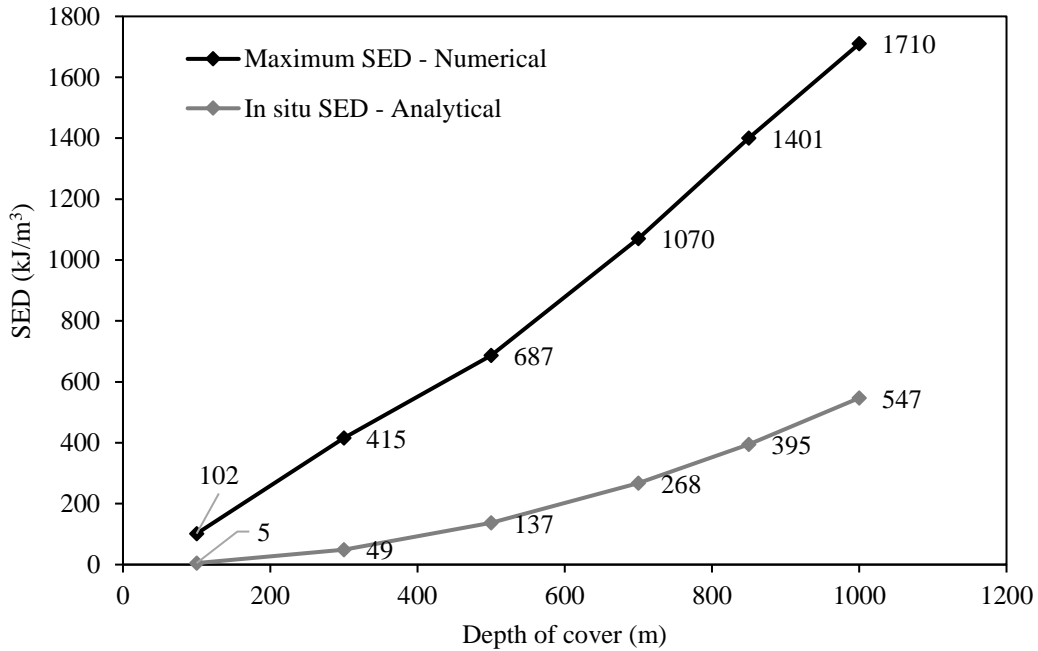
Figure 6: The maximum SED at various mining depths ahead of LW face

Strain energy density during roadway development

Figure 7 shows an example of the energy density contours in the coal seam at the ribs in 700 m depth of mining. The maximum SED point is approximately 5.5 m behind the rib with a magnitude of 338 kJ/m^3. The coal mass between the maximum SED point and the rib face is generally in a yielded state. The average SED in the yielded coal is approximately 44.1 kJ/m^3 in the model shown in **Figure 7**.
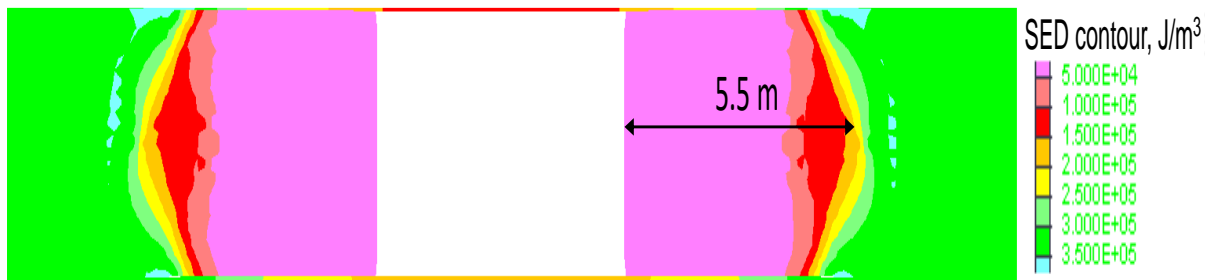

Figure 7: An example of energy density contours in the coal seam at the ribs for development at 700m mining depth

For the development roadway models, the average SED in the yielded coal seam at ribs at various mining depths is shown in **Figure 8**. It shows that the average SED in yielded coal increases from 6 kJ/m^3 in 100 m depth of mining to 51.4 kJ/m^3 in 1000 m depth of mining. The average SED in 1000 m mining depth is approximately 8.5 times the average SED in 100 m mining depth.

Similarly, the maximum SED and its position are summarised in **Figure 10** and **Figure 9**, respectively. As shown in **Figure 9**, with increasing mining depth, the position of maximum SED has the same increasing trend as at a longwall face. The distance increases almost linearly from 0.1 m to 7.6 m when the mining depth increases from 100 m to 1000 m.

As shown in **Figure 10**, the difference between the SED after roadway excavation and the SED at *in situ* stress state increases with increasing mining depth. The magnitude of the maximum SED increases from approximately 6 kJ/m^3 to 780 kJ/m^3 when the mining depth increases from 100 m to 1000 m. The maximum SED equals the average SED in the yielded coal face in 100 m mining depth in roadway. Then, the maximum SED increases to approximately fifteen times the average SED in the yielded coal when depth of mining increases to 1000 m. Furthermore, the difference between the magnitude of the maximum SED and the average SED increases with increasing depth of mining for roadway scenarios.

Similarly, as shown in **Figure 8**, the yielded coal at development rib has much smaller strain energy compared to the coal area with the maximum SED. Thus, the strain energy stored in the elastic coal is also highly likely the main energy source when strain bursts occur in the development scenario.
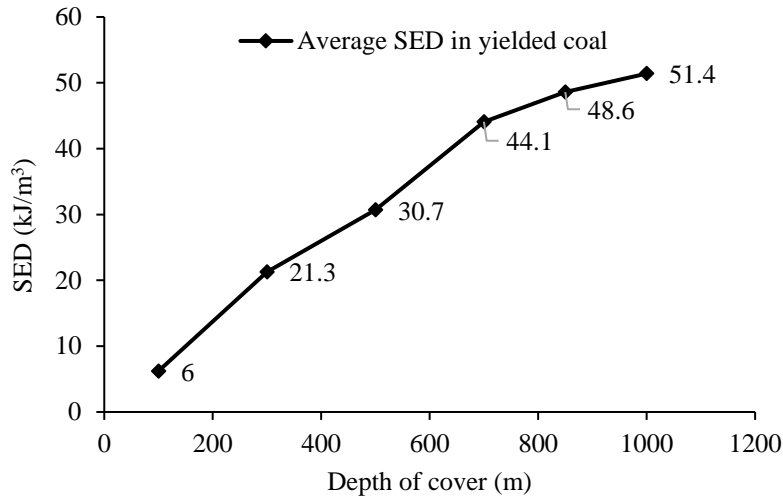

Figure 8: Average SED in yielded coal seam at various mining depths at development ribs
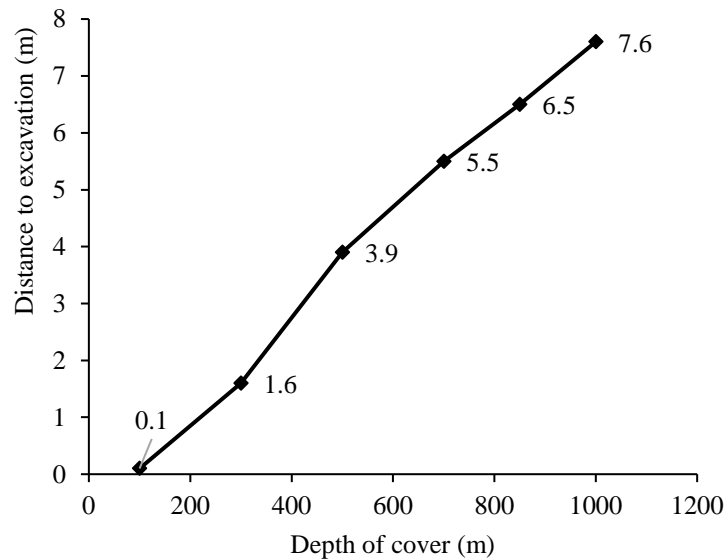

Figure 9: The position of maximum SED at ribs for development roadway

It is of note that the maximum SED around roadway ribs is smaller than that around a longwall face at the same mining depth, as the longwall face carries much more abutment load due to the stress redistribution after longwall excavations. However, the difference between the maximum SED in longwall face and roadway decreases with increasing depth of mining. In 100 m depth of mining, the maximum SED of longwall face is sixteen times the maximum SED of the roadway. This number decreases to two times when the depth of mining increases to 1000 m.

As shown in **Figure 11**, for both development and longwall retreat, the maximum SED migrates deeper with increasing mining depth. However, the rates of the migration are different for the two excavation scenarios. For development, the maximum SED migrates gradually into the coal face. In comparison, for the longwall retreat, the position of the maximum SED migrates from 3 m to 7.7 m into the coal face when the depth of mining increases from 100 m to 700 m. Then, from 700 m to 1000 m depth of mining, the maximum SED rarely migrates into the coal, although the magnitude of the maximum SED still remains at the same increasing rate. The maximum SED increases approximately 700 kJ/m^3 (from 1070

kJ/m³ to 1710 kJ/m³) while the position of the maximum SED remains approximately the same, resulting in higher coal burst risks.
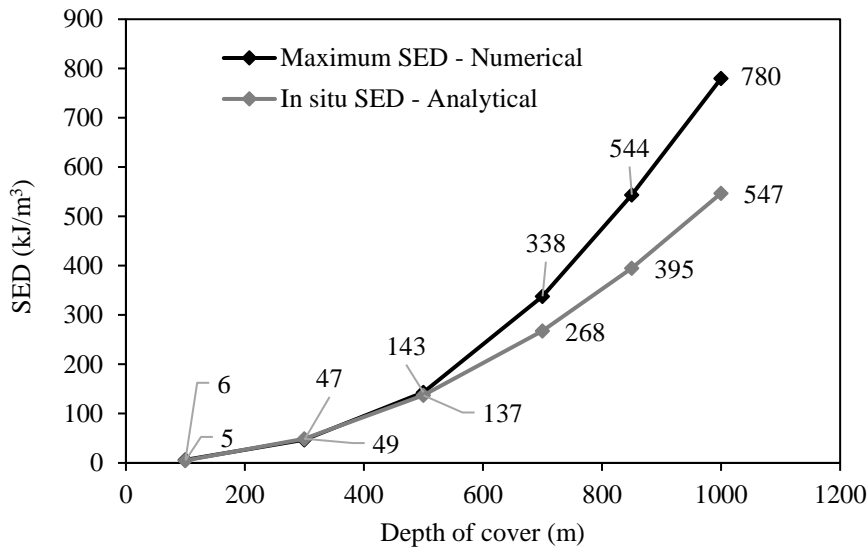

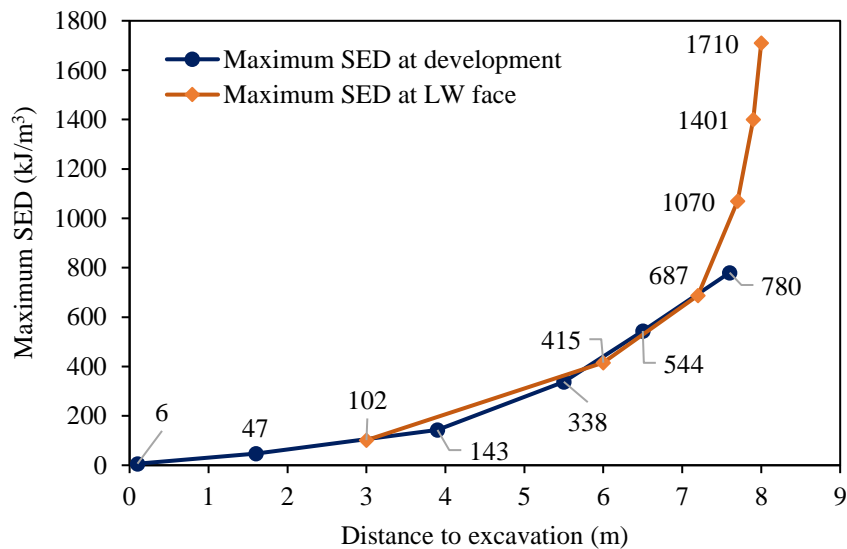**Figure 10: The maximum SED at various mining depths at ribs for development**

Figure 11: Maximum SED and its position in development and longwall face

It is worth noting that in quantifying the strain energy, many factors are involved in the process due to complex underground environmental conditions. The model outputs, e.g., the magnitude and positions of the average and maximum SED, can change significantly in different underground excavation configurations. It is, therefore, necessary to examine the energy changes on a case-by-case basis for a specific condition.

CONCLUSIONS

In this study, the Universal Distinct Element Code (UDEC) is applied to investigate strain energy density distribution in coal excavations. The distance between the maximum strain energy density (SED) area and the coal face increases with increasing mining depth for both development and longwall retreat. The magnitude of SED around the longwall face is greater than that in development. Based on the model configuration in this study, the maximum SED of longwall face and development are 1710 kJ/m³ and 780 kJ/m³, respectively, in 1000 m depth of mining. The average SED in the yielded coal at the coal face is

much less than the maximum SED. Thus, the elastic strain energy stored in the elastic coal is highly likely one of the main energy sources when strain bursts occur. The parametric analyses can deepen the understanding of energy changes and the associated coal burst risks for different mining conditions.

REFERENCE

Galvin, J, 2016. Ground Engineering–Principles and Practices for Underground Coal Mining (Springer).

Hebblewhite, B and Galvin, J, 2017. A review of the geomechanics aspects of a double fatality coal burst at Austar Colliery in NSW, Australia in April 2014, International Journal of Mining Science and Technology, 27 (1), 3-7.

Iannacchione, A and Tadolini, S C, 2016. Occurrence, prediction, and control of coal burst events in the US, International Journal of Mining Science and Technology, 26 (1), 39-46.

Lorig, L and Varona, P, 2013. Guidelines for numerical modelling of rock support for mines, in Proceedings Seventh International Symposium on Ground Support in Mining and Underground Construction, pp 81-105 (Australian Centre for Geomechanics).

Shen, B, Dlamini, B, Chen, L, Duan, Y, Luo, X, Werken, M V D, Vardar, O and Canbulat, I, 2019. Predict stress state and geotechnical conditions near major geological structures using microseismic technology and distinct element modelling. Australian Coal Industry's Research Program (ACARP) Project C26053.

Vardar, O, 2019. Assessment of effects of geological and geotechnical factors on coal burst proneness, PhD thesis, University of New South Wales, Sydney.

Vardar, O, Zhang, C, Canbulat, I and Hebblewhite, B, 2018. A semi-quantitative coal burst risk classification system, International Journal of Mining Science and Technology, 28 (5), 721-727.

Wang, H, Poulsen, B A, Shen, B, Xue, S and Jiang, Y, 2011. The influence of roadway backfill on the coal pillar strength by numerical investigation, International Journal of Rock Mechanics and Mining Sciences, 48 (3), 443-450.

Wei, C, Zhang, C and Canbulat, I, 2020. Numerical analysis of fault-slip behaviour in longwall mining using linear slip weakening law, Tunnelling and Underground Space Technology, 104, 103541.

Wei, C, Zhang, C, Canbulat, I and Huang, W, 2021. Numerical investigation into impacts of major fault on coal burst in longwall mining–A case study, International Journal of Rock Mechanics and Mining Sciences, 147, 104907.

Zhang, C, Canbulat, I, Hebblewhite, B and Ward, C R, 2017. Assessing coal burst phenomena in mining and insights into directions for future research, International Journal of Coal Geology, 179, 28-44.

Zipf, K, 2006. Numerical modelling procedures for practical coal mine design, in Proceedings Golden Rocks 2006, 41st US Symposium on Rock Mechanics (USRMS), Golden, Colorado (American Rock Mechanics Association).